ARTICLE

Transfer-Printing and Host–Guest Properties of 3D Supramolecular Particle Structures

Xing Yi Ling,[†] In Yee Phang,[‡] David N. Reinhoudt,[†] G. Julius Vancso,[‡] and Jurriaan Huskens*[,†]

Molecular Nanofabrication Group and Materials Science and Technology of Polymers, MESA$^+$ Institute for Nanotechnology, University of Twente, P.O. Box 217, 7500 AE Enschede, The Netherlands

ABSTRACT Mechanically robust and crystalline supramolecular particle structures have been constructed by decoupling nanoparticle assembly and supramolecular glue infiltration into a sequential process. First, β-cyclodextrin (CD)-functionalized polystyrene particles ($d \sim 500$ nm) were assembled on a CD-functionalized surface via convective assembly to form highly ordered, but mechanically unstable, particle crystals. Subsequently, the crystals were infiltrated by a solution of adamantyl-functionalized dendrimers, functioning as a supramolecular glue to bind neighboring particles together and to couple the entire particle crystal to the CD surface, both in a noncovalent manner. The supramolecular particle crystals are highly robust, as witnessed by their ability to withstand agitation by ultrasonication. When assembled on a poly(dimethylsiloxane) (PDMS) stamp, the dendrimer-infiltrated particle crystals could be transfer-printed onto a CD-functionalized target surface. By variation of the geometry and size of the PDMS stamps, single particle lines, interconnected particle rings, and V-shaped particle assemblies were obtained. The particle structures served as 3D receptors for the binding of (multiple) complementary guest molecules, indicating that the supramolecular host functionalities of the particle crystals were retained throughout the fabrication process.

KEYWORDS: soft lithography • particle assembly • supramolecular chemistry • host–guest chemistry • transfer printing

INTRODUCTION

Particle assemblies with well-defined morphologies and dimensions are of high interest because of their potentials in optical, electronic, and sensing applications (1). The assembly of individual particles into ordered particle assemblies allows the amplification of their collective physical and/or chemical properties and the emergence of new properties. In addition, mechanical robustness of such particle structures ensures that their function can be exerted on matrixes for long-term applications, e.g., in miniaturized optical (1), electronic (2), and biological (3) devices.

Among the existing particle assembly approaches, the chemically directed assembly of particles is particularly promising in conferring mechanical stability to the particle structures without affecting their structural (and, therefore, physical) properties. The use of electrostatic interactions (4–8), covalent bonding (9, 10), coordination chemistry (11), and biomolecular (12, 13) and supramolecular chemistry (14–18) provides specific coupling chemistries to direct the functionalized particles to complementarily functionalized surfaces, resulting in stable particle layers. For example, Hammond et al. have modulated the charge density of surfaces to control the packing order and density of multicomponent particle arrays via electrostatic and hydrophobic interactions (19). In several cases, the coupling chemistry has been integrated with physical particle assembly techniques to improve the packing density of the particle structures. Physical particle assembly techniques (20, 21), such as capillary assembly (7, 22–26), sedimentation (27), and Langmuir–Blodgett techniques (28), are known to fabricate highly crystalline and packed particle structures when assembling unfunctionalized particles, but generally without inferring stability, by utilizing surface tension and long-range attractive forces. In general, a high affinity between chemically functionalized particles and the target substrate reduces the mobility of the particles and thus leads to less ordered structures (29). Hence, a compromise between the surface–particle interactions and the physical assembly process is needed to achieve highly stable and ordered particle crystals when using a single-step directed assembly approach.

The integration of particles into devices typically requires their placement in specific positions. Top-down nanofabrication techniques, e.g., microcontact printing (μCP) (30), transfer printing (31–34), nanoimprint lithography (35, 36), and photolithography (26), have been combined with the self-assembly of particles to direct the particles into desired patterns with specified dimensions. Recently, μCP has been extended to the transfer printing of various nanostructures (33, 37, 38). Wolf et al. have demonstrated the transfer printing of nanoparticles with a single 60-nm-particle resolution (31, 32). In many cases, only a single layer of particles has been transferred in each step because the transfer printing was carried out via conformal contact. Hence, the success of the printing strongly depends on the adhesion (e.g., van der Waals interactions) between the transferred objects and the target surface (38).

* To whom correspondence should be addressed. E-mail: J.Huskens@utwente.nl.

Received for review February 3, 2009 and accepted March 16, 2009

[†] Molecular Nanofabrication Group.

[‡] Materials Science and Technology of Polymers.

DOI: 10.1021/am900071y

Published on Web 04/08/2009

Scheme 1. Formation of 3D Supramolecular Particle Crystals on CD Monolayers

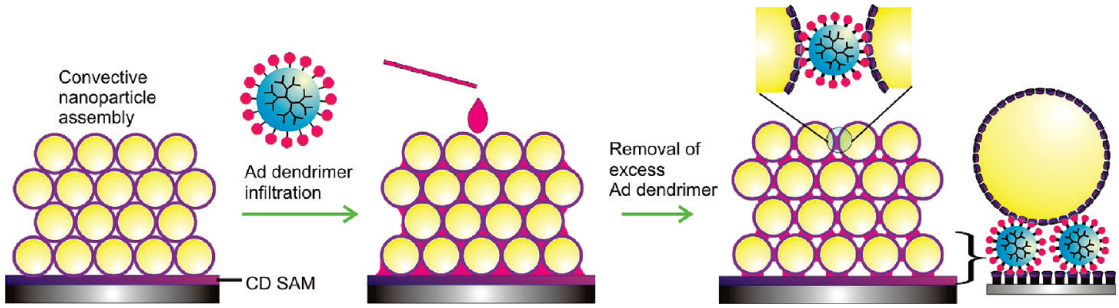

Our group has explored supramolecular β-cyclodextrin (CD) host–guest chemistry for the directed and specific assembly of particle structures. CD-functionalized particles were assembled onto (patterned) CD monolayers, with guest-functionalized dendrimers as a noncovalent supramolecular glue (18, 35, 39–41). To date, the nanoparticle structures were directly assembled onto a surface with complementary recognition properties. Fine-tuning of the binding strength of the host–guest interactions is needed during the particle assembly to result in nearly hexagonally close-packed (hcp) and stable particle arrays (29).

Here, a new strategy of forming 3D supramolecular particle structures with macroscopic robustness and improved order is demonstrated. In this strategy, the nanoparticle assembly and supramolecular binding of nanoparticles are decoupled, resulting in a sequential fabrication process. At first, particles are physically assembled to form ordered particle crystals without mechanical stability. Subsequently, stability is induced to the particle crystal by infiltration with supramolecular glues to bind neighboring particles in a stable entity. In a preliminary communication (42), this procedure was followed to create free-standing particle structures. In the current study, the mechanical robustness of thus-assembled particle crystals was assessed by sonication in water. By incorporation of the sequential processes with transfer printing, 3D-patterned particle crystals of various shapes and dimensions have been transferred from elastomeric poly(dimethylsiloxane) (PDMS) stamps onto target CD-covered substrates via host–guest interactions. The recognition functionality of the supramolecular particle crystals has been investigated by studying the binding of complementary guest molecules. As a proof of principle, the specific binding of lissamine rhodamine-labeled divalent guest molecules into the particle structures is demonstrated.

RESULTS AND DISCUSSION

Ordered and stable supramolecular 3D particle crystals were created on surfaces by applying convective particle assembly and supramolecular host–guest chemistry in a sequential manner (Scheme 1). CD-functionalized polystyrene (PS-CD) particles (29) were physically assembled and organized onto CD monolayers (Chart 1) by using a capillary-assisted deposition setup (35, 43). The preformed CD-functionalized particle array was subsequently infiltrated with complementary adamantyl-terminated poly(propylene imine) dendrimers of generation 5 [G5-PPI-$(Ad)_{64}$] (44) and rinsed with a 10 mM CD solution to remove an excess of dendrimers from the particle crystal.

In order to assess the effect of dendrimer infiltration on the stability of the particle array, the substrate was sonicated in water for 10 min. Figure 1 shows the scanning electron microscopy (SEM) images of the particle crystals after sonication, where part A was infiltrated with G5-PPI-$(Ad)_{64}$ and part B was a sample without infiltration. The SEM image of Figure 1A clearly indicates that the neighboring particles were attached to each other and that the entire particle crystal was robustly attached to the surface via infiltration of G5-PPI-$(Ad)_{64}$ dendrimers. The crystal remained hcp on the CD monolayer, which is indicated by a 2D Fourier transform in the inset of Figure 1A. In contrast, the particle array without G5-PPI-$(Ad)_{64}$ infiltration was completely destroyed by sonication, with only a few particles remaining on the surface. These results underline the importance of infiltration with adamantyl-terminated dendrimers to infer stability to the particle arrays. The strong and thermodynamically stable multivalent host–guest interactions between G5-PPI-$(Ad)_{64}$ and PS-CD allow the dendrimer to function as a supramolecular glue to chemically bind neighboring particles together into a large particle structure and to adhere the particle structure to the CD monolayer. The order of the particle structures achieved here contrasts with the direct assembly of CD-functionalized particles onto CD monolayers preadsorbed with adamantyl- or ferrocenyl-terminated dendrimers, which typically resulted in less than perfectly packed particle arrays (29, 35, 41, 45). The current method optimally exploits the advantages of convective assembly in ordering particles and of supramolecular interactions in binding particles into a stable entity, by applying them in a sequential manner, and thus allows the formation of highly ordered and stable functionalized particle crystals.

It is not necessary that the assembly and integration of particles are carried out directly onto the final substrate. An elastomeric PDMS stamp was used as a temporary substrate, which, after dendrimer infiltration, allows the transfer printing of the complete particle structures onto a target surface (Scheme 2). PS-CD particles were convectively assembled into the grooves of variously shaped oxidized PDMS stamps (Scheme 2). The stamps were dipped in a 1 mM aqueous solution of G5-PPI-$(Ad)_{64}$ for 30 min, after which they were blown dry with N_2. The PDMS stamps with G5-PPI-$(Ad)_{64}$-

Chart 1. Chemical Structures of Adamantyl-Terminated Poly(propylene imine) Dendrimers of Generation 1 [G1-PPI-$(Ad)_4$], a Monolayer of CD on SiO_2, Lissamine Rhodamine-Labeled Divalent Adamantyl Guest 1, Native Lissamine Rhodamine, and Fluorescein-Labeled Divalent Adamantyl Guest 2

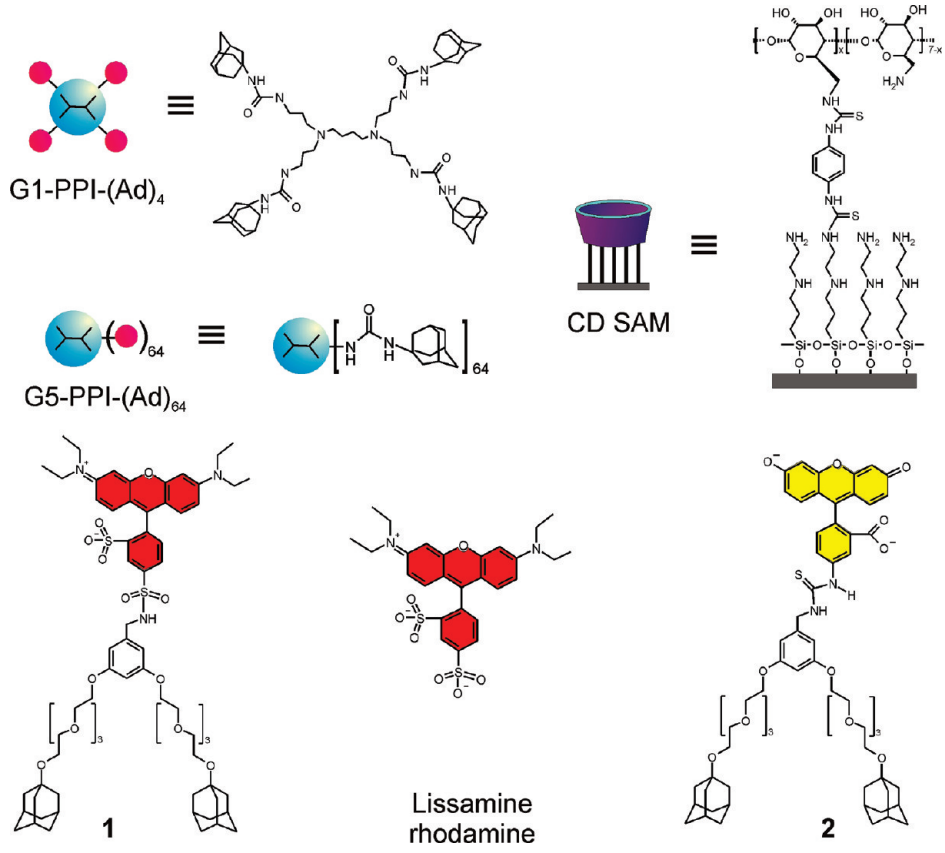

infiltrated PS-CD particles were brought into conformal contact with target substrates functionalized with a CD monolayer in a high-humidity environment. After stamp removal, the substrates were thoroughly rinsed with water and blown dry with N_2.

Long and continuous micrometer-sized particle lines were successfully transferred from an appropriately shaped PDMS stamp onto a CD monolayer on silicon (Figure 2A,B). The width of the printed structures was 3 μm, which is in agreement with the width of the grooves of the PDMS stamp. The height of the printed microstructures is similar to that of the original template and corresponds to two layers of particles being transferred (Figure 2C,D). Some cracks were observed on the printed particle structures, probably resulting from drying after the transfer-printing process. A zoom-in SEM image (Figure 2B) reveals that the packing of the transferred particle building blocks remained highly ordered and hcp, with a quality similar to that of the particle crystal shown in Figure 1A. Compared to physical transfer-printing schemes reported before (28, 32), which permit only single-layered particle printing, the supramolecular glue infiltration process described here ensures the cross-linking of multi-layered particle crystals into stable entities and, therefore, allows the simultaneous transfer printing of 3D multilayered particle crystals.

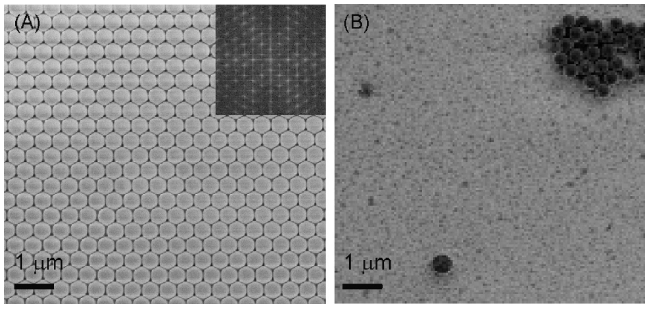

FIGURE 1. SEM images of particle crystals with (A) and without (B) infiltration with G5-PPI-$(Ad)_{64}$ after sonication in water. The inset at the upper right of part A shows the 2D Fourier transform of part A.

It should be mentioned that the humidity of the printing environment is particularly vital to the success of transfer printing of the supramolecular particle structures. Under ambient conditions, the transfer was less effective; i.e., transfer occurred only in some areas of the sample. The efficient printing in a humid environment (yield >90%) is attributed to the fact that CD host–guest interactions are most favored in the presence of water. A similar observation was reported before in the case of supramolecular metal transfer printing (46).

To assess the effect of infiltration by G5-PPI-$(Ad)_{64}$ on the particle transfer printing, a PS-CD array was directly printed on a CD monolayer without infiltration, which resulted in the printing of less than one layer of individual particles in the contact area (Figure 3A). This indicates that the use of a

Scheme 2. Preparation of Multilayered PS-CD Particle Structures on Variously Patterned PDMS Stamps and the Transfer Printing of These Structures onto CD Monolayer Substrates[a]

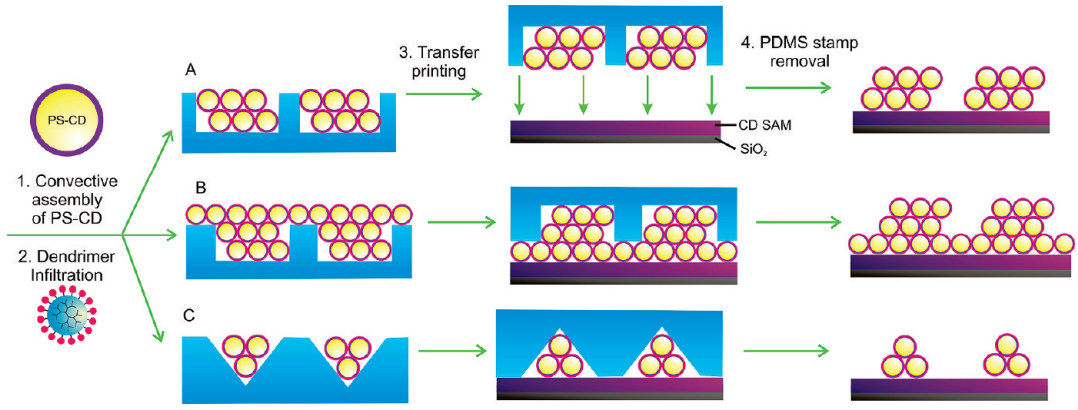

[a] The shape and geometry of the resulting particle crystals can be varied by the choice of the shape and size of the PDMS stamps (A and C) and the withdrawal speed of the convective assembly step (A and B).

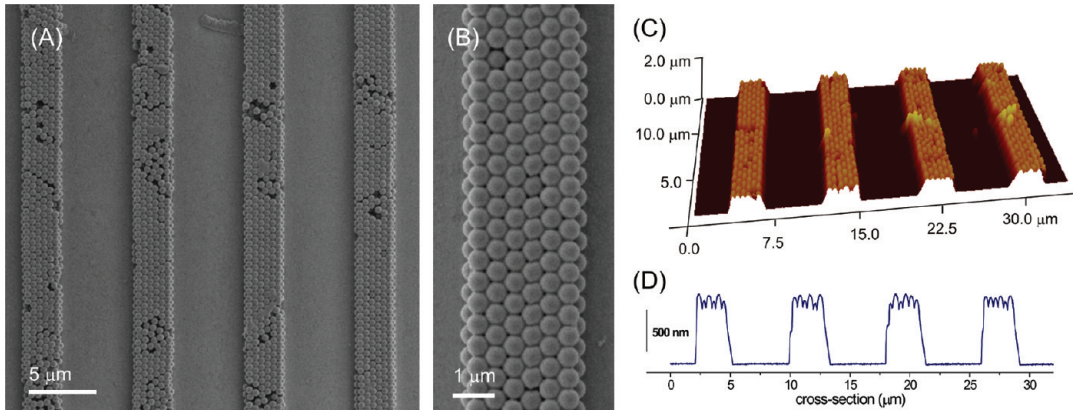

FIGURE 2. SEM (A and B) and AFM (C) images and an AFM height profile (D) of the transfer-printed 3D continuous particle crystals [infiltrated with G5-PPI-$(Ad)_{64}$] on CD monolayers on SiO_2 substrates.

supramolecular glue is crucial in bonding the particles into a stable particle structure and in ensuring good adhesion to the target CD monolayer via multiple host–guest interactions.

In order to separate the interactions between the particles and the substrate from the internal particle–particle cohesion, a PS-CD structure without dendrimer infiltration was transfer-printed onto a G5-PPI-$(Ad)_{64}$-preadsorbed CD monolayer substrate. Well-defined line features, but less orderly packed single layers of particles, were obtained (Figure 3B–D). The other particles remained on the PDMS stamp, probably as a result of adhesion between the PDMS surface and the particles (31). The bilayer particle structures on the PDMS stamp apparently have broken apart during the printing process, so that only the particles with direct contact to the surface were successfully transferred.

One of the degrees of freedom when using supramolecular host–guest interactions is the binding strength and stoichiometry. In particular, the number of interactions and the resulting multivalent binding strength of adamantyl dendrimers binding to CD surfaces are a function of the dendrimer generation (47). We have used adamantyl-terminated poly(propylene imine) dendrimer of generation 1 [G1-PPI-$(Ad)_4$, Chart 1], which has only 4 adamantyl end groups as compared to the 64 end groups of G5-PPI-$(Ad)_{64}$, as a weaker supramolecular glue in the transfer printing of 3D particle structures. The transfer printing of G1-PPI-$(Ad)_4$-infiltrated particles onto a CD monolayer showed that mostly only a single layer of PS-CD was transferred, with occasionally a few particles stacked on top of this layer (Figure 3E). These results show that the binding of G1-PPI-$(Ad)_4$ is not strong enough to integrate the discrete particles into a stable macroscopic structure. Hence, it is important to use supramolecular glue with a sufficiently high binding strength. In this case, G5-PPI-$(Ad)_{64}$ efficiently binds the particles into a stable crystal.

To demonstrate the versatility of the supramolecular transfer-printing process, particles were assembled onto a PDMS stamp, in this case not only in the grooves but also across the entire stamp (Scheme 2B). This was achieved by lowering the substrate withdrawal speed during the convective assembly step. The 3D and continuous particle array was then infiltrated with G5-PPI-$(Ad)_{64}$ and printed onto a CD monolayer. As shown in Figure 4, a large 3D and continuous patterned particle structure was printed on the surface. The printed structure inherited the good hcp order (Figure 4B) from the initial particle array on PDMS. As dictated by the depth of the grooves on the stamp, the protruding ridges were two particle layers high (Figure 4C,D). As is also seen in Figure 4, the underlying full particle layer

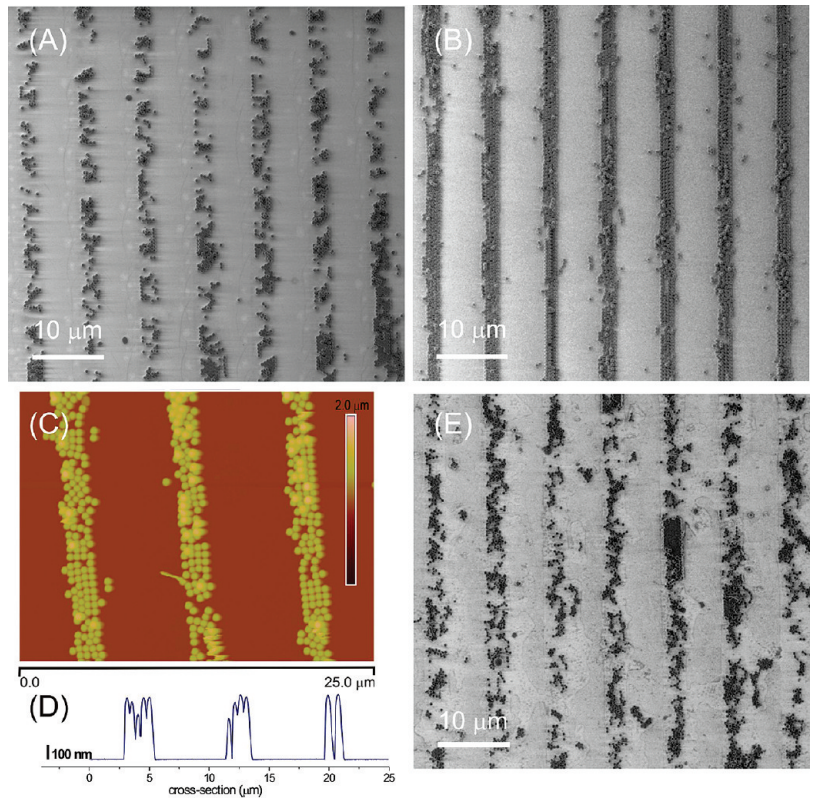

FIGURE 3. SEM image after transfer printing of a PS-CD structure without dendrimer infiltration onto a CD monolayer (A). SEM (B) and AFM (C) images and an AFM height profile (D) of a PS-CD nanostructure (without dendrimer infiltration) after transfer printing onto a G5-PPI-$(Ad)_{64}$-coated CD monolayer. SEM image of a PS-CD particle structure infiltrated with G1-PPI-$(Ad)_4$, after transfer printing onto a CD monolayer (E).

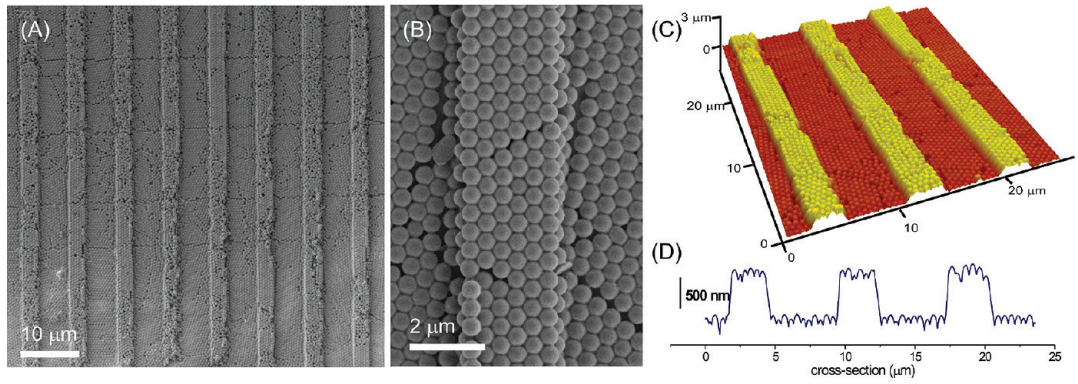

FIGURE 4. SEM images of a transfer-printed patterned continuous particle crystal [infiltrated with G5-PPI-$(Ad)_{64}$] on a CD monolayer substrate (A and B). 3D AFM image (C) and an AFM height profile (D) of the printed particle structure.

shows domain boundaries and does not follow the crystal axes of the ridges.

By manipulation of the sizes and shapes of the patterns on the PDMS stamp (Scheme 2), a broad range of transfer-printed particle structures was made (Figure 5). On a PDMS stamp with grooves of 500 nm and 1 and 2 μm wide and a depth of 150 nm, single-layer particle lines were printed onto CD monolayer substrates (Figure 5A–C). When using the 500-nm structures, the position of some particle lines was slightly shifted, which is attributed to the deformation of the soft PDMS during the printing process and reduced mechanical strength of the particle structure. Nevertheless, the configurations of the particle lines are well retained. As is shown in Figure 5D,E, networks of interconnected PS-CD particle rings were printed onto CD monolayers. The particles remained hcp-ordered upon printing. There were occasionally unoccupied spaces within the networks, which can be due to defects originating from the convective assembly step. Parts F and G of Figure 5 shows V-shaped particle crystals printed on a surface, which were made using stamps with V-shaped grooves (Scheme 2C). On the basis of the results of the supramolecular transfer printing, the control over the shape and size of the particle assemblies can be provided at will by carefully selecting proper building blocks and stamps of desired shapes and dimensions.

To investigate the host–guest functionality of the generated PS-CD microstructures, lissamine rhodamine-labeled divalent adamantyl guest molecules (**1**; Chart 1) were mi-

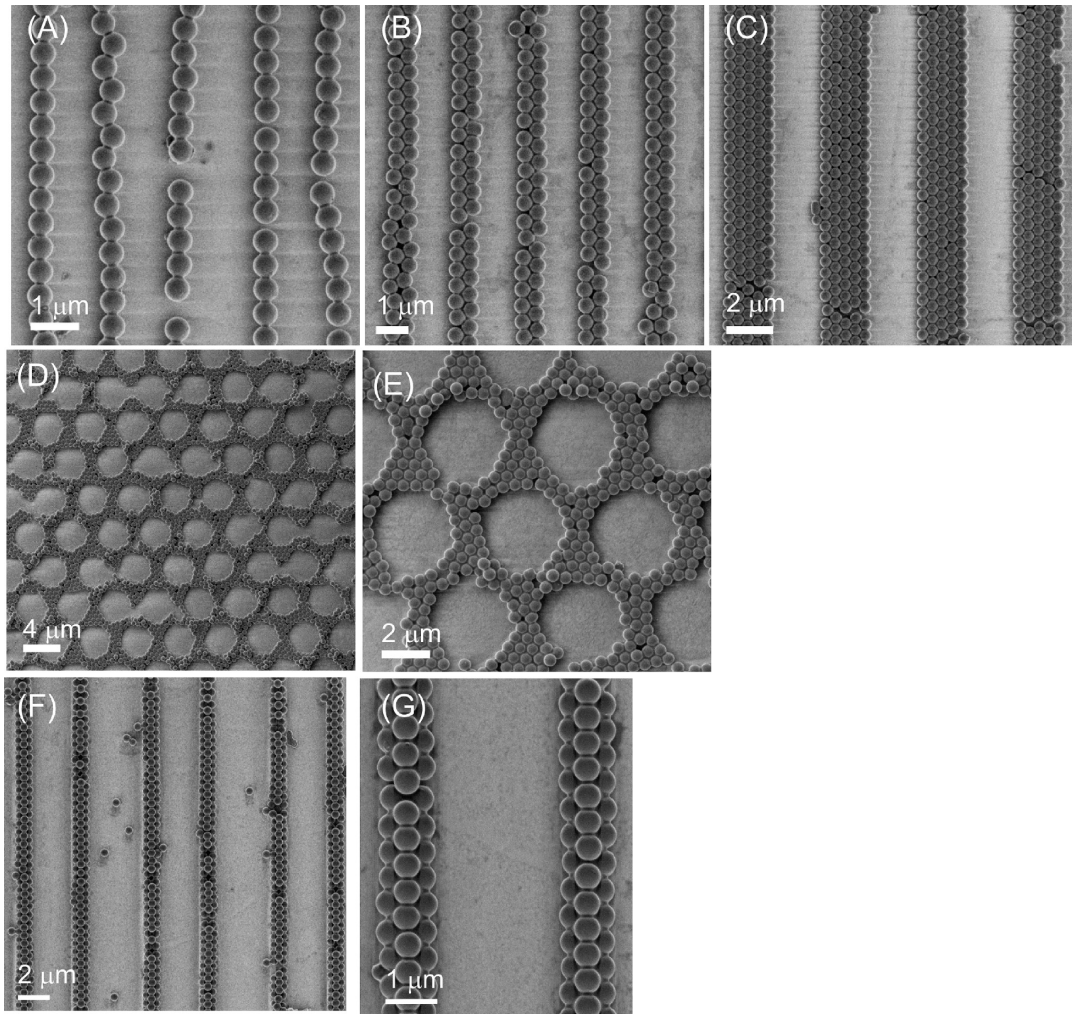

FIGURE 5. SEM images of the transfer-printed particle crystals of different shapes on CD monolayer substrates: single-layer particle lines from a stamp with grooves of 500 nm (A), 1 μm (B), and 2 μm (C) in width, single-layer networks of interconnected PS-CD particle rings (D and E), and double-layer V-shaped particle crystals made according to Scheme 2C (F and G).

Scheme 3. Microcontact Printing of Lissamine Rhodamine-Labeled Divalent Adamantyl Guest 1 on a Transfer-Printed Particle Structure and Subsequent Rinsing

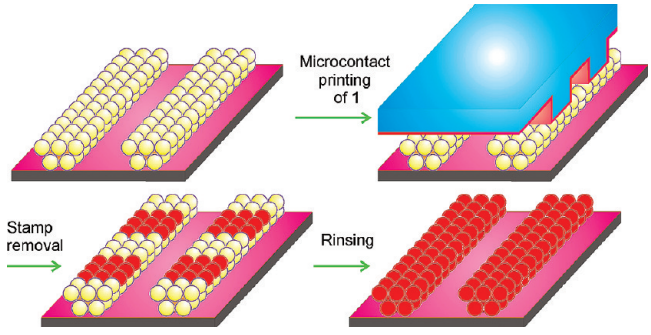

crocontact-printed perpendicularly onto the continuous particle lines (Scheme 3). These divalent guest molecules are known to bind to CD monolayers via divalent host–guest interactions (48). A fluorescence image (Figure 6A) shows the substrate after printing **1** onto the particle lines. The image shows predominantly fluorescent squares, equivalent to the size of the contact area between the particle structure and the PDMS stamp. After intense rinsing with a CD solution at pH 2, the fluorescence became apparent along the complete particle lines (Figure 6B), while in the areas outside the particle crystals, the intensity remained negligible. The integrated fluorescence intensity along the particle lines remained constant, indicating diffusion of **1** along the particle lines, with negligible desorption. Upon rinsing with 1 M NaOH, the fluorescence intensity (Figure 6C) remained similar. This indicates that the stability of the interaction is not resulting from electrostatic interactions because NaOH is expected to deprotonate the dendrimer cores and to eliminate this interaction. To confirm this, native lissamine rhodamine, which is not a guest molecule for CD, was printed onto particle line structures (Figure 6D). The fluorescent molecules remained on the particle crystal after rinsing with a CD solution at pH 2 (Figure 6E), probably as a result of electrostatic interactions, but fluorescence was completely removed by 1 M NaOH (Figure 6F). This indicates that the supramolecular host properties of the particle crystals were retained after the transfer-printing process. These results differ from the direct printing of **1** on flat CD monolayers, where copious rinsing with a CD solution resulted in (near-)complete reduction in fluorescence (48).

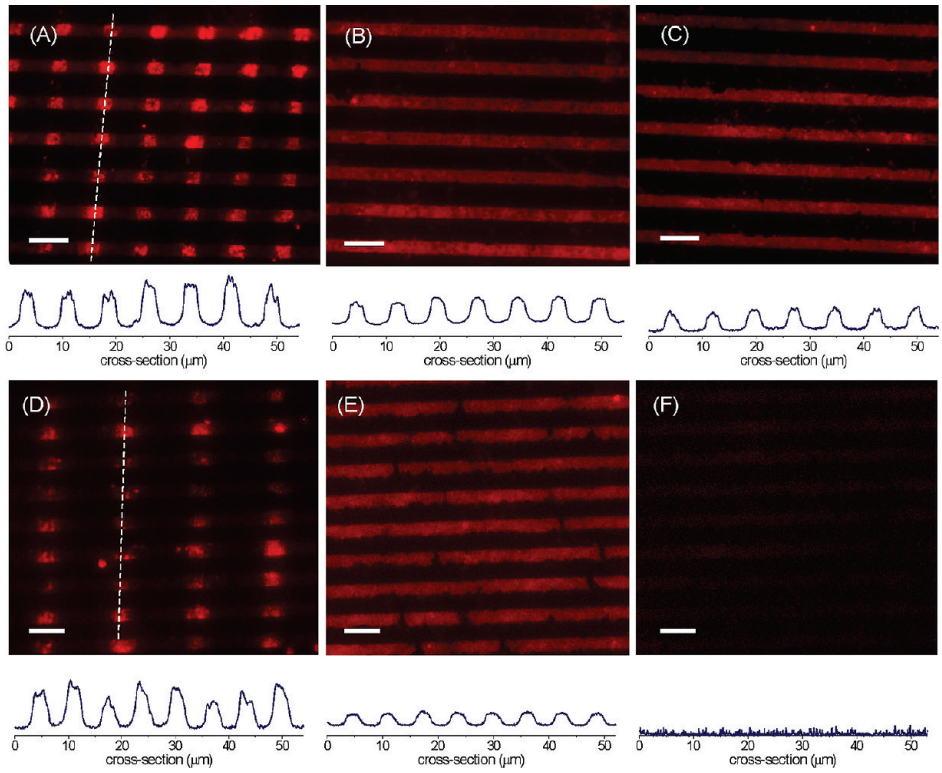

FIGURE 6. Fluorescence microscopy images and intensity profiles of the printing of divalent adamantyl guest 1 (A−C) and native lissamine rhodamine (D−F) on infiltrated and transfer-printed particle structures before (A and D) and after rinsing with a CD solution at pH 2 (B and E) and subsequent rinsing with 1 M NaOH (C and F). The images were taken at green excitation light. All scale bars indicate 10 μm. The white dashed lines indicated the areas where fluorescence profiles were taken. All fluorescence intensity profiles are shown at the same scale.

This difference may be attributed to the 3D nature of the particle crystal. These results therefore suggest that the particle crystal lines can act as 3D receptors, which allow the transportation of complementary guest molecules within their structure. An in-depth study on the dynamics of the guest molecules within the particle crystal is out of the scope of this report.

The potential of the particle crystals as building blocks for multiple guest molecule storage and transportation was further examined by using **1** and an analogous divalent guest **2**, labeled with fluorescein. A drop of fluorescein-labeled divalent adamantyl guest **2** was casted on a substrate with transfer-printed particle structures, freshly printed with **1** (Figure 7A) and subsequently rinsed with water. Imaging with green excitation light (Figure 7B) showed that the discrete fluorescent squares of **1** had developed into homogeneously fluorescent lines. Imaging the substrate with blue excitation (Figure 7E) showed that **2** was immobilized along the same particle structures, also in a homogeneous fashion. Similar to the results discussed above, rinsing with a CD solution at pH 2 (Figure 7C,F) and 1 M NaOH (Figure 7D,G) did not reduce the fluorescence intensities in either case. The combined results show that multiple guest molecules can be stored within the CD-functionalized particle crystals simultaneously via the specific divalent host−guest interactions.

CONCLUSIONS

Stable and ordered supramolecular particle crystals were prepared by decoupling the steps of convective particle assembly and supramolecular glue infiltration of particles in a sequential manner. The particle crystals infiltrated with supramolecular glues are highly robust and able to withstand agitation by ultrasonication. When this process was performed on PDMS stamps, 3D multilayered particle crystals were transfer-printed onto a target substrate via supramolecular interactions. Our strategy demonstrates the potential of high-precision positioning of such mechanically robust 3D particle crystals onto a specific target surface. The sizes and shapes of the transfer-printed supramolecular particle crystals can be tuned by the design of the PDMS templates and the conditions of the convective assembly.

Such stable and ordered particle crystals with recognition functionalities open up new routes for bottom-up fabrication of miniaturized micro- and nanostructures for applications in sensing and photonic devices. The core material of the particles can be of arbitrary materials (e.g., metallic, inorganic, or organic) to suit the specific application. In particular, the supramolecular properties of the individual particles can potentially be employed as sensing channels for the detection, storage, and transportation of (multiple) complementary molecules or nanoparticles.

EXPERIMENTAL SECTION

Materials. β-Cyclodextrin (CD) heptamine, adamantyl-terminated poly(propylene imine) dendrimers of generation 1 and 5 [G1-PPI-$(Ad)_4$ and G5-PPI-$(Ad)_{64}$], the lissamine rhodamine, and fluorescein-labeled divalent adamantyl guests (**1** and **2**) were synthesized as described before (44, 48, 49). *N*-[3-(Trimethoxysilyl)propyl]ethylenediamine, 1,4-phenylene diisothio-

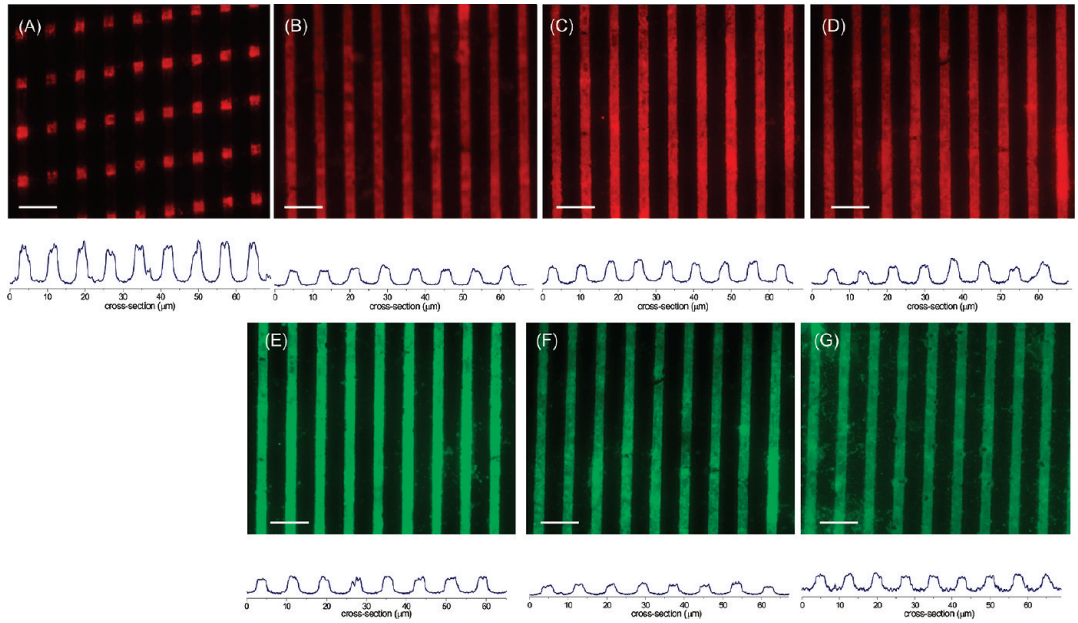

FIGURE 7. Fluorescence microscopy images and intensity profiles of the printing of lissamine rhodamine divalent guest 1 on infiltrated and transfer-printed particle structures (A), after the addition of fluorescein-labeled divalent guest 2 and rinsing with water (B and E), and after subsequent rinsing with a CD solution at pH 2 (C and F) and rinsing with 1 M NaOH (D and G). The images at the top (A–D) were taken at green excitation light, whereas the images at the bottom (E–G) were taken at blue excitation. All scale bars indicate 10 μm. All fluorescence intensity profiles are shown at the same scale.

cyanate, and lissamine rhodamine B sulfonyl chloride were obtained from Sigma Aldrich. Poly(dimethylsiloxane) (PDMS) Sylgard 184 prepolymer and curing agent were obtained from Dow Corning. Carboxylate-functionalized polystyrene particles of 500 nm were purchased from Polysciences Inc. CD-functionalized polystyrene (PS-CD) particles were prepared from these as described before (29). Milli-Q water with a resistivity higher than 18 MΩ · cm was used in all experiments.

Substrate and Monolayer Preparation. Silicon substrates were cleaned by immersion in piranha solution (concentrated H_2SO_4 and 33% H_2O_2 in a 3:1 volume ratio; ***Warning!*** *Piranha should be handled with caution; it is a highly corrosive oxidizing agent!*) for 15 min to form a SiO_2 layer on the surface. The substrates were then sonicated in Milli-Q water and ethanol for 1 min and dried with N_2. CD monolayers were obtained according to a published procedure (16, 50). In brief, the substrates were functionalized with *N*-[3-(trimethoxysilyl)propyl]ethylenediamine by gas-phase evaporation. Transformation of the amino-terminated self-assembled monolayers to isothiocyanate-bearing layers was accomplished by exposure to an ethanolic solution of 1,4-phenylene diisothiocyanate at 50 °C for 2 h. CD monolayers were finally obtained by the reaction of isothiocyanate-terminated monolayers with CD heptamine in water at pH 7.5, at 50 °C for 2 h.

The patterned silicon masters were made by photolithography followed by reactive ion etching or e-beam lithography. They consisted of gratings of 5 μm lines at a 8 μm period with a height of 750 nm; a stamp consisted of 1 and 2 μm grooves with a height of 150 nm, of 2 μm dots with a height of 500 nm, of 2 μm V-shaped grooves with a height of 760 nm, and of 5 μm lines at a 20 μm period with a height of 2 μm. PDMS stamps were prepared by casting a 10:1 (v/v) mixture of PDMS prepolymer and curing agent against a patterned silicon master. After curing of the stamps overnight, they were mildly oxidized in an O_2 plasma etcher (Tepla 300E) for 1 min to render them hydrophilic.

Assembly of PS-CD Particle Layers/Arrays. A particle array was prepared by depositing PS-CD particles onto a CD monolayer or an oxidized PDMS stamp by capillary-assisted deposition at a withdrawal speed between 0.1 and 1 μm/s (35, 43). The preformed particle array was then gently dipped in a 1 mM aqueous solution of G1-PPI-$(Ad)_4$ or G5-PPI-$(Ad)_{64}$ for 30 min, followed by rinsing with water and blow drying with N_2.

Transfer Printing of Particle Structures. An oxidized PDMS stamp with dendrimer-infiltrated PS-CD particle structures was brought into conformal contact with a CD monolayer, unless otherwise stated. The printing was performed on a platform of a close-by water bath at 40 °C. When the particle printing was performed in ambient conditions without humidity control, the transfer of the particle structures was less effective and took a long printing time (3 h). At high humidity, only 1 h of printing time was sufficient to induce successful transfer printing with higher yields. The printing time was not further optimized. After removal of the stamp, the substrates were thoroughly rinsed with water and blown dry with N_2.

Printing of Divalent Guest 1 or Native Lissamine Rhodamine on Transfer-Printed Particle Structures. An oxidized PDMS stamp with 5 μm lines at a 20 μm period with a height of 2 μm was inked by soaking in a 10 μM aqueous solution of **1** for 2 min. The stamps were blown dry in a stream of N_2 before printing. The stamps were brought into conformal contact with printed particle structures (3 or 4 μm particle line structure at a 8 μm period) for 2 min and then carefully removed. The substrate was subsequently rinsed with a 10 mM CD solution at pH 2 and 1 M NaOH, respectively.

Binding of Divalent Guest 2 to Transfer-Printed Particle Structures. A drop of a 10 μM aqueous solution of **2** was cast onto particle line structures, which had been freshly printed with **1**. After 2 min, the particle structure was rinsed with water, a 10 mM CD solution at pH 2, and 1 M NaOH, respectively. Fluorescence images were taken after each rinsing step.

SEM. All SEM images were taken with a HR-LEO 1550 FEF SEM.

AFM. AFM measurements were carried out with a Dimension D3100 using a NanoScope IVa controller equipped with a hybrid 153 scanner (Veeco/Digital Instruments (DI), Santa Barbara, CA) under ambient conditions. Silicon cantilevers from Nanosensors (Nanosensors, Wetzlar, Germany) were used for intermittent contact (tapping) mode operation.

Fluorescence Microscopy. Fluorescence microscopy was performed using an Olympus IX71 inverted research microscope equipped with a mercury burner U-RFL-T as the light source and a digital camera Olympus DP70 (12.5-million-pixel cooled digital color camera) for image acquisition. Green excitation light and red emission light ($510 \leq \lambda_{ex} \leq 550$ nm; $\lambda_{em} \geq 590$) and blue excitation and green emission light ($450 \leq \lambda_{ex} \leq 480$ nm; $\lambda_{em} \geq 515$ nm) were filtered using a U-MWG Olympus filter cube.

Acknowledgment. Yiping Zhao, Janet Acikgoz, and Iwan Heskamp are gratefully acknowledged for providing the lithographically patterned masters. X.Y.L and J.H. thank the Council for Chemical Sciences of The Netherlands Organization for Scientific Research (NWO-CW) for financial support (Vidi Vernieuwingsimpuls Grant 700.52.423 to J.H.).

REFERENCES AND NOTES

(1) Arsenault, A.; Fournier-Bidoz, S.; Hatton, B.; Miguez, H.; Tetreault, N.; Vekris, E.; Wong, S.; Yang, S. M.; Kitaev, V.; Ozin, G. A. *J. Mater. Chem* **2004**, *14*, 781.
(2) Yablonovitch, E. *Sci. Am.* **2001**, *285*, 46.
(3) Katz, E.; Willner, I. *Angew. Chem., Int. Ed.* **2004**, *43*, 6042.
(4) Decher, G.; Hong, J. D.; Schmitt, J. *Thin Solid Films* **1992**, *210*, 831.
(5) Blonder, R.; Sheeney, L.; Willner, I. *Chem. Commun.* **1998**, 1393.
(6) Hicks, J. F.; Seok-Shon, Y.; Murray, R. W. *Langmuir* **2002**, *18*, 2288.
(7) Fustin, C. A.; Glasser, G.; Spiess, H. W.; Jonas, U. *Langmuir* **2004**, *20*, 9114.
(8) Zheng, J. W.; Zhu, Z. H.; Chen, H. F.; Liu, Z. F. *Langmuir* **2000**, *16*, 4409.
(9) Li, D.; Zhang, Y. J.; Jiang, J. G.; Li, J. H. *J. Colloid Interface Sci.* **2003**, *264*, 109.
(10) Granot, E.; Patolsky, F.; Willner, I. *J. Phys. Chem. B* **2004**, *108*, 5875.
(11) Shenhar, R.; Jeoung, E.; Srivastava, S.; Norsten, T. B.; Rotello, V. M. *Adv. Mater.* **2005**, *17*, 2206.
(12) Maye, M. M.; Nykypanchuk, D.; van der Lelie, D.; Gang, O. *J. Am. Chem. Soc.* **2006**, *128*, 14020.
(13) Shenton, W.; Pum, D.; Sleytr, U. B.; Mann, S. *Nature (London)* **1997**, *389*, 585.
(14) Zirbs, R.; Kienberger, F.; Hinterdorfer, P.; Binder, W. H. *Langmuir* **2005**, *21*, 8414.
(15) Boal, A. K.; Ilhan, F.; DeRouchey, J. E.; Thurn-Albrecht, T.; Russell, T. P.; Rotello, V. M. *Nature (London)* **2000**, *404*, 746.
(16) Ling, X. Y.; Reinhoudt, D. N.; Huskens, J. *Langmuir* **2006**, *22*, 8777.
(17) Wanunu, M.; Popovitz-Biro, R.; Cohen, H.; Vaskevich, A.; Rubinstein, I. *J. Am. Chem. Soc.* **2005**, *127*, 9207.
(18) Crespo-Biel, O.; Dordi, B.; Reinhoudt, D. N.; Huskens, J. *J. Am. Chem. Soc.* **2005**, *127*, 7594.
(19) Zheng, H. P.; Lee, I.; Rubner, M. F.; Hammond, P. T. *Adv. Mater.* **2002**, *14*, 569.
(20) Ozin, G. A.; Yang, S. M. *Adv. Funct. Mater* **2001**, *11*, 95.
(21) Dziomkina, N. V.; Hempenius, M. A.; Vancso, G. J. *Adv. Mater.* **2005**, *17*, 237.
(22) Denkov, N. D.; Velev, O. D.; Kralchevsky, P. A.; Ivanov, I. B.; Yoshimura, H.; Nagayama, K. *Nature (London)* **1993**, *361*, 26.
(23) Malaquin, L.; Kraus, T.; Schmid, H.; Delamarche, E.; Wolf, H. *Langmuir* **2007**, *23*, 11513.
(24) Jiang, P.; Bertone, J. F.; Hwang, K. S.; Colvin, V. L. *Chem. Mater.* **1999**, *11*, 2132.
(25) Park, S. H.; Xia, Y. *Langmuir* **1999**, *15*, 266.
(26) Yin, Y.; Lu, Y.; Gates, B.; Xia, Y. *J. Am. Chem. Soc.* **2001**, *123*, 8718.
(27) Vlasov, Y. A.; Bo, X.-Z.; Sturm, J. C.; Norris, D. J. *Nature (London)* **2001**, *414*, 289.
(28) Santhanam, V.; Andres, R. P. *Nano Lett.* **2004**, *4*, 41.
(29) Ling, X. Y.; Malaquin, L.; Reinhoudt, D. N.; Wolf, H.; Huskens, J. *Langmuir* **2007**, *23*, 9990.
(30) Park, J. I.; Lee, W. R.; Bae, S. S.; Kim, Y. J.; Yoo, K. H.; Cheon, J.; Kim, S. *J. Phys. Chem. B* **2005**, *109*, 13119.
(31) Kraus, T.; Malaquin, L.; Delamarche, E.; Schmid, H.; Spencer, N. D.; Wolf, H. *Adv. Mater.* **2005**, *17*, 2438.
(32) Kraus, T.; Malaquin, L.; Schmid, H.; Riess, W.; Spencer, N. D.; Wolf, H. *Nat. Nanotechnol.* **2007**, *2*, 570.
(33) Meitl, M. A.; Zhu, Z. T.; Kumar, V.; Lee, K. J.; Feng, X.; Huang, Y. Y.; Adesida, I.; Nuzzo, R. G.; Rogers, J. A. *Nat. Mater.* **2006**, *5*, 33.
(34) Liao, J.; Bernard, L.; Langer, M.; Schönenberger, C.; Calame, M. *Adv. Mater.* **2006**, *18*, 2444.
(35) Maury, P.; Péter, M.; Crespo-Biel, O.; Ling, X. Y.; Reinhoudt, D. N.; Huskens, J. *Nanotechnology* **2007**, *18*, 044007.
(36) Maury, P.; Escalante, M.; Reinhoudt, D. N.; Huskens, J. *Adv. Mater.* **2005**, *17*, 2718.
(37) Meitl, M. A.; Zhou, Y.; Gaur, A.; Jeon, S.; Usrey, M. L.; Strano, M. S.; Rogers, J. A. *Nano Lett.* **2004**, *4*, 1643.
(38) Shir, D. J.; Jeon, S.; Liao, H.; Highland, M.; Cahill, D. G.; Su, M. F.; El-Kady, I. F.; Christodoulou, C. G.; Bogart, G. R.; Hamza, A. V.; Rogers, J. A. *J. Phys. Chem. B* **2007**, *111*, 12945.
(39) Nijhuis, C. A.; Huskens, J.; Reinhoudt, D. N. *J. Am. Chem. Soc.* **2004**, *126*, 12266.
(40) Mahalingam, V.; Onclin, S.; Peter, M.; Ravoo, B. J.; Huskens, J.; Reinhoudt, D. N. *Langmuir* **2004**, *20*, 11756.
(41) Ling, X. Y.; Reinhoudt, D. N.; Huskens, J. *Chem. Mater.* **2008**, *20*, 3574.
(42) Ling, X. Y.; Phang, I. Y.; Maijenburg, W.; Schönherr, H.; Reinhoudt, D. N.; Vancso, G. J.; Huskens, J. *Angew. Chem., Int. Ed.* **2009**, *48*, 983.
(43) Ling, X. Y.; Phang, I. Y.; Reinhoudt, D. N.; Vancso, G. J.; Huskens, J. *Int. J. Mol. Sci.* **2008**, *9*, 486.
(44) Michels, J. J.; Baars, M.; Meijer, E. W.; Huskens, J.; Reinhoudt, D. N. *J. Chem. Soc., Perkin Trans. 2* **2000**, 1914.
(45) Crespo-Biel, O.; Dordi, B.; Maury, P.; Péter, M.; Reinhoudt, D. N.; Huskens, J. *Chem. Mater.* **2006**, *18*, 2545.
(46) Nijhuis, C. A.; ter Maat, J.; Bisri, S. Z.; Weusthof, M. H. H.; Salm, C.; Schmitz, J.; Ravoo, B. J.; Huskens, J.; Reinhoudt, D. N. *New J. Chem.* **2008**, *32*, 652.
(47) Huskens, J.; Deij, M. A.; Reinhoudt, D. N. *Angew. Chem., Int. Ed.* **2002**, *41*, 4467.
(48) Mulder, A.; Onclin, S.; Péter, M.; Hoogenboom, J. P.; Beijleveld, H.; ter Maat, J.; Garcia-Parajo, M. F.; Ravoo, B. J.; Huskens, J.; Van Hulst, N. F.; Reinhoudt, D. N. *Small* **2005**, *1*, 242.
(49) Beulen, M. W. J.; Bügler, J.; Lammerink, B.; Geurts, F. A. J.; Biemond, E.; van Leerdam, K. G. C.; van Veggel, F. C. J. M.; Engbersen, J. F. J.; Reinhoudt, D. N. *Langmuir* **1998**, *14*, 6424.
(50) Onclin, S.; Mulder, A.; Huskens, J.; Ravoo, B. J.; Reinhoudt, D. N. *Langmuir* **2004**, *20*, 5460.

AM900071Y